Acta Cryst. (1984). B40, 139–145

Structure and Disorder of Dicalcium Barium Cyclopropanecarboxylate

BY K. STADNICKA

Faculty of Chemistry, Jagiellonian University, ul. Karasia 3, 30–060 *Kraków, Poland*

AND A. M. GLAZER

*Clarendon Laboratory, Parks Road, Oxford OX*1 3*PU, England*

(*Received* 24 *August* 1983; *accepted* 10 *October* 1983)

Abstract

The crystal structure of the prototype phase of dicalcium barium cyclopropanecarboxylate is described. $Ca_2Ba[(CH_2)_2CHCOO]_6$, $M_r = 728$, cubic, $Fd3m$ (O_h^7), $a = 18{\cdot}409\ (9)$ Å, $V = 6239$ Å^3, $Z = 8$, $D_x = 1{\cdot}55$, $D_m = 1{\cdot}56\ (1)$ Mg m^{-3}; $R = 0{\cdot}034$, $R_w = 0{\cdot}032$ and $R_G = 0{\cdot}037$ for 516 reflections. As in the isomorphous compound dicalcium barium propionate, the structure is disordered with the organic groups statistically in two sites related by a pseudomirror plane. X-ray diffuse scattering measurements show that there are correlated locally ordered regions in the form of platelets perpendicular to ⟨100⟩ and elongated along the ⟨110⟩ directions, corresponding to regions of opposite chiralities. The correlation lengths are found to be 23·4 (5) Å projected along [110] and 4·1 (1) Å projected along [001]. It has been found that at room temperature the crystal is normally orthorhombic, but that X-ray dosage stabilizes the prototype phase at this temperature. The orthorhombic–cubic transition in the absence of X-ray dosage is at about 308 K.

Introduction

As part of an extensive study of the relationship between the physical properties and crystal structures of dicalcium metal propionates, Stadnicka & Glazer (1980) published an account of the structure and disorder of dicalcium barium propionate, DBP. It was found that the space group was $Fd3m$ (O_h^7) and that the twofold axes of this space group implied a statistical two-site disorder of the propionate group about its long axis (it is important to note that we use the term 'disorder' here in the general sense of either static or dynamic disorder, as structure determination alone cannot distinguish the two). X-ray diffuse scattering studies revealed streaks in the $h > 0$, $k > 0$, $l > 0$ quadrant directed along $[1\bar{1}0]$ (and in its symmetry-equivalent directions in other quadrants of reciprocal space), whose cross-sections were more elongated along [001] than along [110]. These streaks were found to pass through all reciprocal-lattice positions in the $hk0$ plane given by $h + k = 8n$. Diffractometer measurements by Singh & Glazer (1981) showed that the profile cross-sections along [110] and [001] could be described very closely by the simple one-dimensional disorder model of Wilson (1962), applied independently to each direction, to give short-range correlation lengths of 24·5 (5) and 4·6 (1) Å respectively. The disorder was interpreted in terms of approximately two-dimensional 'platelets' of local order of opposite chiralities (in this connection note that $Fd3m$ contains both 4_1 and 4_3 axes).*

A structural study of the Sr salt, DSP, at room temperature (Glazer, Stadnicka & Singh, 1981) confirmed these ideas, since the structure was of a single chirality, $P4_12_12$ (D_4^4), and it was possible to use the positions of Ca and Sr to explain the anisotropic temperature factors of Ca and Ba in DBP in terms of a superposition of chiral states produced by $P4_12_12 \oplus P4_32_12 \otimes$ threefold rotations about cubic [111]. A low-temperature structural study by Stadnicka, Glazer, Singh & Śliwiński (1982) enabled the spontaneous polarization of DSP in its ferroelectric phase to be calculated.

Optical simulations of the diffuse scattering in DBP by Welberry (1982) gave additional support to the disorder model proposed and demonstrated that the cations produced the major contribution to the diffuse intensity.

At the same time, we have tried to produce entirely new materials of this type to see what the effect would be of changing the organic group in the crystal. Crystals of dicalcium metal acrylates (Stadnicka & Glazer, 1982) were grown and, in particular, the Ba compound DBA was found to have a phase transition from an orthorhombic phase of space group $Pnma$ (D_{2h}^{16}) or $Pn2_1a$ (C_{2v}^9) to a cubic phase of space group $Fd3m$ (O_h^7) at about 382 K. On the basis of this work we were able to propose a scheme for all the known phases found in these materials (Fig. 1).

In the present paper we describe work on a new compound of the series, DBC. Cyclopropanecarboxylic acid was chosen because the molecule is

* A fuller discussion of this model can be found in Glazer, Stadnicka & Singh (1981).

0108-7681/84/020139-07$01.50

similar in size and shape to the disordered propionate group in DBP, *viz*:

Preliminary work

Crystals of DBP were grown by slow evaporation of an aqueous solution of the cyclopropanecarboxylate salts in stoichiometric proportions. The resulting crystals were optically clear and highly reflective, and approximately octahedral in shape, similar in appearance to DBA (Stadnicka & Glazer, 1982).

Between crossed polars some evidence for anisotropic optical extinction was found, but not very clearly. The crystals showed a mottled appearance with some regions dark and others light, as if they were of poor quality, despite their excellent appearance in ordinary light. However, on heating to above 308 K good isotropic extinction was observed suggesting a phase transition to a cubic phase near this temperature. On cooling the crystals to liquid-nitrogen temperatures the extinction became sharp and anisotropic, confirming this view of a phase transition above room temperature. Hence, the mottled effect referred to above results from the crystals at room temperature being at just below the transition temperature and has nothing to do with crystal quality.

X-ray Weissenberg photographs taken with Cu $K\alpha$ radiation showed that the unit cell can be described by $a = b = c$, $\alpha = \beta = \gamma = 90°$ to within the resolution permitted by the camera. The diffraction pattern was similar to that of DBP, except that there were some weak extra reflections on $hk0$ of the type $h + k \neq 4n$. The diffraction spots were exceptionally sharp and the whole pattern indicated that the crystal was of unusually high quality. After several days of exposure to X-rays, it was noticed that the extra reflections had disappeared and the remaining pattern, which was still very sharp, could be indexed as $Fd3m$ (O_h^7). Optical examination of the crystal showed it to be isotropic, and hence we concluded that X-ray dosage had stabilized the high-temperature phase at room temperature. (It would be interesting to establish how low in temperature one could go and still see this unusual effect.)

Low-temperature Guinier–Simon photographs of powdered DBC were taken over the range 113 to 323 K. It was seen that several of the high-temperature cubic lines were split at very low temperatures just as in DBA, but to a smaller extent. Recent X-ray work by Singh & Wondre (1984) on DBP shows a similar transition at about 268 to 263 K. From this we see that all three Ba compounds probably undergo the same type of transition (with the order of transition temperatures given by DBP < DBC < DBA) from the prototype $Fd3m$ (O_h^7) phase to a ferroelastic phase of symmetry $Pnma$ (D_{2h}^{16}) or $Pn2_1a$ (C_{2v}^9), and therefore belong to the Aizu (1969) ferroic species $m3mFmmm(ss)$ or $m3mFm2m(ss)$. The extra reflections found in fresh DBC crystals therefore arise from the fact that at room temperature before heavy X-ray dosage they are in the orthorhombic phase. On the basis of these results DBC has been added to the scheme in Fig. 1.

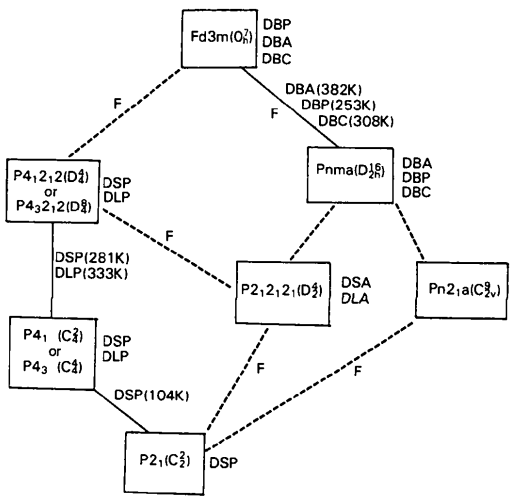

Fig. 1. Schematic diagram of successive phases for the dicalcium metal propionates, acrylates and carboxylates. The full lines indicate known transitions and dashed lines potential continuous phase transitions, so far unreported. The letter *F* denotes a ferroelastic phase transition.

Crystal structure of prototype phase

(*a*) *Experimental*

A single crystal of natural shape approximately 0·20 × 0·27 × 0·29 mm was mounted along [001]. After several days of exposure to Mo $K\alpha$ radiation at room temperature, Weissenberg photographs showed no $hk0$ reflections with $h + k \neq 4n$, thus confirming that the crystal was in its prototype phase.

This crystal was then used for X-ray intensity measurement on a Stoe Stadi-2 diffractometer with graphite-monochromated Mo $K\alpha$ radiation produced with a Philips PW 1730. The cubic unit cell was refined by least squares from the 2θ angles of 15 measured high-angle reflections.

Data were collected on ten reciprocal-lattice layers ($l = 0, \ldots, 9$). *F* centring was assumed in accordance with the Weissenberg reflections. In each layer a check reflection was measured after every 20 reflections; in general the variation was less than 2%. Between each layer measurement the intensities of the 800 and 080 reflections were checked to eliminate intensity drift with time. Lorentz–polarization corrections were

Table 1. *Fractional coordinates, thermal parameters and bond lengths and angles*

(*a*) Fractional coordinates (daggers indicate atoms given site-occupancy factor of one-half) and temperature factors (Å^2) {$T = \exp[-2\pi^2(U_{11}h^2a^{*2} + 2U_{12}hka^*b^* + \ldots)]$}

	Site	Point symmetry	x	y	z	U_{11}	U_{22}	U_{33}	U_{23}	U_{13}	U_{12}
Ba	8(*a*)	$\bar{4}3m$	0	0	0	0·0346 (2)	U_{11}	U_{11}	0	0	0
Ca	16(*c*)	$\bar{3}m$	$\frac{1}{8}$	$\frac{1}{8}$	$\frac{1}{8}$	0·0679 (5)	U_{11}	U_{11}	−0·0215 (4)	U_{23}	U_{23}
O	96(*g*)	*m*	0·1536 (2)	0·0394 (1)	0·0394 (1)	0·139 (3)	0·102 (1)	U_{22}	−0·048 (2)	0·001 (11)	U_{13}
C(1)	48(*f*)	*mm*	0·1883 (3)	0	0	0·050 (2)	0·076 (2)	U_{22}	0·003 (3)	0	0
C(2)†	96(*g*)	*m*	0·2655 (4)	−0·0188 (3)	−0·0188 (3)	0·047 (3)	0·131 (4)	U_{22}	−0·021 (5)	−0·001 (2)	U_{13}
C(3)†	192(*h*)	1	0·3175 (4)	−0·0110 (4)	0·0432 (4)	0·083 (3)	0·239 (6)	0·164 (5)	−0·007 (5)	−0·050 (4)	−0·008 (4)

(*b*) Bond lengths (Å) and angles (°) – compared with DBP

	DBC	DBP		DBC	DBP
Ba–Ca	3·986 (2)	3·936 (1)	Ca–O–Ba	96·7 (1)	97·0 (2)
Ba–O	3·008 (4)	2·965 (5)	O–C(1)–O′	116·1 (5)	115·5 (8)
Ca–O	2·289 (3)	2·253 (4)	O′–C(1)–C(2)	140·9 (5)	139·0 (8)
O–O′	2·054 (6)	2·039 (8)	O–C(1)–C(2)	103·0 (5)	105·6 (7)
O–C(1)	1·210 (4)	1·205 (5)	C(1)–C(2)–C(3)	114·0 (5)	113 (1)
C(1)–C(2)	1·502 (9)	1·57 (2)	C(3)–C(2)–C(3′)	56·2 (3)	—
C(2)–C(3)	1·497 (8)	1.36 (2)	C(3′)–C(3)–C(2)	61·9 (3)	—
C(3)–C(3′)	1·41 (10)	—			

applied and common reflections on even and odd layers showed that no arbitrary scale factors between layers were needed. In all 2489 reflections were measured. Absorption corrections ($\mu_{Mo\,K\alpha} = 15{\cdot}39\ cm^{-1}$) were made with the *SHELX*76 program (Sheldrick, 1976), with maximum and minimum transmission factors of 0·783 and 0·764. It was found that all $hk0$ reflections with $h + k \neq 4n$ had intensities less than 4σ and so they were omitted.

(*b*) *Refinement*

After merging the data according to point group $m3m$ ($R = 0{\cdot}009$), 571 independent reflections resulted. Of these, 55 with $F_o < 4\sigma(F_o)$ were omitted to give 516 independent reflections. Scattering factors for neutral atoms were assumed [taken from *International Tables for X-ray Crystallography* (1974, p. 99; f' and f'' from p. 149)].

As the structure was expected to be isomorphous with DBP, the Ba, Ca and O ions were taken to be in the special positions

Ba	8(*a*)	0,	0,	0
Ca	16(*c*)	$\frac{1}{8}$,	$\frac{1}{8}$,	$\frac{1}{8}$
O	96(*g*)	0·1532,	0·0397,	0·0397.

A Fourier map based on these atoms revealed the positions of the C(1) [48(*f*)] and C(2) [96(*g*)] atoms. This map showed C(2) to be statistically distributed in two positions across the (011) mirror plane and lying in the (01$\bar{1}$) mirror plane. Subsequent difference Fourier maps gave the C(3) positions, which through the disorder inherent in this structure occur in four general positions related by the (011) and (01$\bar{1}$) mirror planes.

After several cycles of refinement (*SHELX*76) with anisotropic temperature factors on all atoms and weights according to $w = k[\sigma^2(F_o) + gF_o^2]^{-1}$, g converged to 0·0001, and the agreement factors were $R = 0{\cdot}034$, $R_w = 0{\cdot}032$ and $R_G = [\sum w(\Delta F)^2 / \sum wF_o^2]^{1/2} = 0{\cdot}037$. A difference map showed that there was no residual electron density greater than 0·1 e Å^{-3} (the H atoms could not be observed because of the large amount of disorder in the structure). The only high correlation was 82% between the scale factor and U_{11} for Ba, as seen in DBP. Table 1 lists the final fractional coordinates and temperature factors.*

(*c*) *Description of the structure*

In Fig. 2 the Ba, Ca and O atoms are shown. The coordination of the cations by O is precisely the same as in DBP [*cf.* Fig. 5 in Stadnicka & Glazer (1980)], that is with 12-fold coordination around Ba and six-fold in the shape of a trigonal antiprism around Ca. From Table 1 we see that all Ba–Ca, Ba–O and Ca–O distances are between 1·3 and 1·6% larger in DBC, despite a 2·2% increase in (density)$^{1/3}$, showing that the Ba–O and Ca–O bond strengths are weaker in this case. This can be seen also in the fact that the distances between O atoms in *different* molecules are significantly larger in DBC than in DBP [2·971 (6) around Ba and 3·48 (1) Å around Ca, *cf.* 2·918 (8) and 3·43 (1) Å]. Other differences between the two structures are the smaller temperature factors (about 32–36%) for Ba and Ca in DBC, and a different orientation of the major axes of the O thermal ellipsoids – in DBP they are directed towards Ca whereas here

* Lists of structure factors have been deposited with the British Library Lending Divison as Supplementary Publication No. SUP 38926 (4 pp.). Copies may be obtained through The Executive Secretary, International Union of Crystallography, 5 Abbey Square, Chester CH1 2HU, England.

they are directed more towards Ba. The large decrease in thermal-ellipsoid magnitudes despite an increase in bond lengths is unusual, as one would expect more thermal amplitude if more space is available: this contrary observation may support the idea that in DBP most of the observed thermal ellipsoid is caused by disorder rather than by normal thermal motion. Clearly in DBC this disorder is less significant. We note that the ellipsoid for Ca is a disc flattened perpendicular to [111], whereas for Ba it is a sphere. The same shapes are found in DBP and were explained by Glazer, Stadnicka & Singh (1981) by superposition of opposite chiral structures, as a result of supposing DBP to consist of chiral microdomains.

In Fig. 3 the organic molecule is shown as a stereoplot and this should be compared with Fig. 6 in the DBP paper. Apart from the cyclopropane ring the most obvious difference is in the O thermal ellipsoids which point along the molecular axis – in DBP they were perpendicular to this axis. This effect is also seen in Fig. 4. In addition C(1) and C(2) look more isotropic when viewed along the molecular axis along [100] for the molecule chosen. It is interesting to note also that in DBC the C(3) atoms lie above and below the molecular plane (Fig. 4*b*), whereas in DBP the whole molecule is planar (Fig. 4*c*). For the particular molecule drawn in Fig. 3 the (011) plane is a pseudomirror to give the statistical two-site disorder of the molecule (not shown in the diagram). The bond lengths and angles are given in Table 1 and can be seen to be similar to those in DBP. The molecular geometry agrees well with that found in *t*-2,*t*-3-dimethyl-*r*-1-cyclopropanecarboxylic acid (Luhan & McPhail, 1972).

In Fig. 4(*a*) are shown the thermal ellipsoids projected onto the molecular plane. The anisotropy of C(1) and O can be explained very well by superimposing two molecules disordered across the (011) plane. C(1), which was refined as a single atom, is in reality two disordered C(1) atoms very close together to give the anisotropy shown in the diagram. By keeping the O–C(1)–O angle as 116° (as in Table 1) and the C(1)–O distances equal we find that each O ellipsoid results from the superposition of two O atoms. The large anisotropy seen in C(2) and C(3) suggests a further disordering or motion in agreement with the view expressed by Glazer, Stadnicka & Singh (1981) that in these types of compound the metal–O–Ca interactions are the overriding features, with the organic parts tightly anchored at the carboxylate end and the C(2), C(3) 'tail' fitting in where it can. As the 'tail' is farthest from the cations it has more room to move about. The view in Fig. 4(*b*) is consistent with an additional rocking of the molecule about its axis. As in DBP, we may suggest that the cyclopropane group oscillates about the molecular axis and occasionally flips over to its alternative site: such a dynamic model is consistent with the magnetic-resonance observations in DBP (Nakamura, Suga, Chihara & Seki, 1968; Bhat, Dhar & Srinivasan, 1982). If true, the two-site disorder described here has a dynamic rather than a static character. It is interesting to note from Fig. 4(*b*) that the two C(3) atoms in DBC correspond *not* to the two disordered C(3) atoms in DBP but to the two extreme positions of one C(3) atom during its oscillation about the molecular axis. The disordered C(3) positions in DBP correspond to the disordering of the *whole* cyclopropane ring in DBC by the pseudomirror plane.

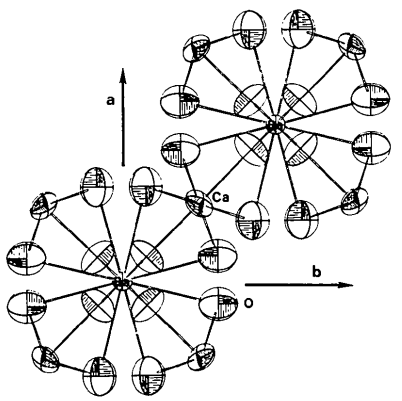

Fig. 2. The coordination of Ba and Ca by O. Thermal ellipsoids are shown for each atom. The cations shown are at positions: Ba 0, 0, 0; Ca $\frac{1}{8}$, $\frac{1}{8}$, $\frac{1}{8}$; and Ba $\frac{1}{4}$, $\frac{1}{4}$, $\frac{1}{4}$ along [111].

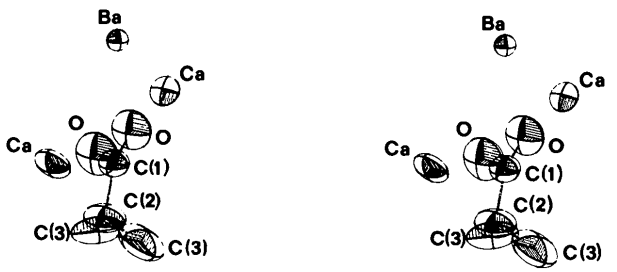

Fig. 3. Stereoplot of the cyclopropanecarboxylate group and neighbouring Ba and Ca.

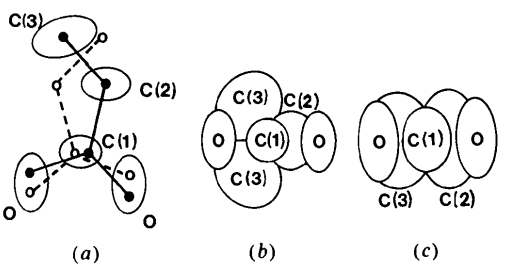

Fig. 4. (*a*) Two cyclopropanecarboxylate groups superimposed to explain the apparent thermal ellipsoids of C(1) and O, as viewed on the molecular plane. (*b*) One cyclopropanecarboxylate group viewed down the molecular axis. (*c*) One propionate group viewed down the molecular axis.

Fig. 5 shows a projection of all the atoms in a slice between $z = 0{\cdot}175 \pm 0{\cdot}125$, and this should be compared with Fig. 4 of Stadnicka & Glazer (1980). The shaded ellipsoids represent those of one molecular fragment ordered according to maximization of the C(3)–C(3) intermolecular contacts. We note that the shortest distance is (2) 3·351 Å, a little shorter than the expected van der Waals distance (the H atoms are above and below the cyclopropane ring and therefore are not so important in determining the intermolecular contacts). Therefore, when compared with distance (3) 3·778 Å we would expect a tendency for the molecules *A* and *F* to adopt an arrangement where distance (3) is more likely to occur, at least over a limited local region of the crystal. Similarly distance (1) 3·627 Å is also short and again would tend to order the molecules *A*, *B*, *C* and *D* as shown. Note, however, that molecule *E* cannot be fixed once *A*, *B*, *C* and *D* are chosen because distance (1) is found for *both* positions of C(3) in *E*. On the other hand, if we order *E* with respect to *A* and *C*, then *B* and *D* cannot be ordered. This demonstrates that local ordering will occur independently in two-dimensional regions (platelets) perpendicular to the three ⟨100⟩ directions. This picture is very similar to that in DBP and results in ordered regions of opposite chiralities. The C(3) intermolecular contacts determine the degree of correlation across the ordered regions through the above mechanism.

X-ray diffuse scattering

X-ray photographs taken with a stationary crystal and unfiltered Cu radiation showed evidence of diffuse streaks rather similar to those found in DBP (Stadnicka & Glazer, 1980; Singh & Glazer, 1981). No noticeable change in the streaks was observed with X-ray dose. It was decided to make a quantitative study of the *hk*0 reciprocal-lattice plane to compare with that for DBP.

The same crystal that was used for the structural work was employed here. With the same diffractometer and radiation, a 0·8 mm collimator and 0·5 × 0·5 mm detector slit at 120 mm from the crystal, intensity measurements were made at steps of resolution $\frac{1}{25}a^*$ and $\frac{1}{4}b^*$. Each point was measured for 90 s. The numbers of counts at each point were rounded off to the nearest 50 and plotted on a large-scale map of the *hk*0 plane, with a value of 100 counts as the cut-off value above background.

The results of this measurement are shown in Fig. 6 which should be compared with Fig. 1 in Singh & Glazer (1981). The diffuse streaks shown in Fig. 6 are weaker than those seen in the DBP paper because a smaller crystal was used for this study. However, it was noticed that the Bragg intensities in DBC were, despite this, considerably stronger in DBC. Nevertheless, it can be seen that along rows given by $|h| + |k| = 8n$ the intensity is elongated in [1$\bar{1}$0] for the upper-right quadrant (and along [110] for the lower-right quadrant), and the pattern is in broad agreement with that found in DBP.

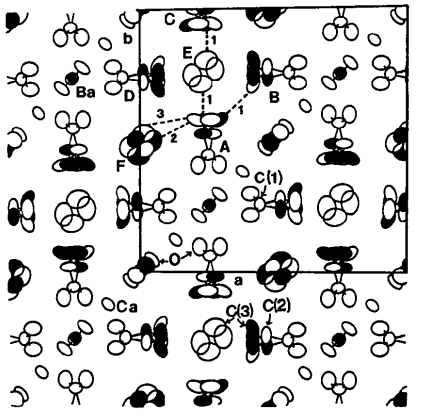

Fig. 5. Projection of a section of the structure on to (001) with $z = 0{\cdot}175 \pm 0{\cdot}125$. Thermal ellipsoids are drawn for each atom with C(2) and C(3) shown in both disordered sites either side of the pseudomirror plane. The shading indicates one ordered arrangement of C(3) and C(2) if it is assumed that intermolecular C(3)–C(3) contacts are maximized. The distances marked are (1) 3·627, (2) 3·351 and (3) 3·778 Å.

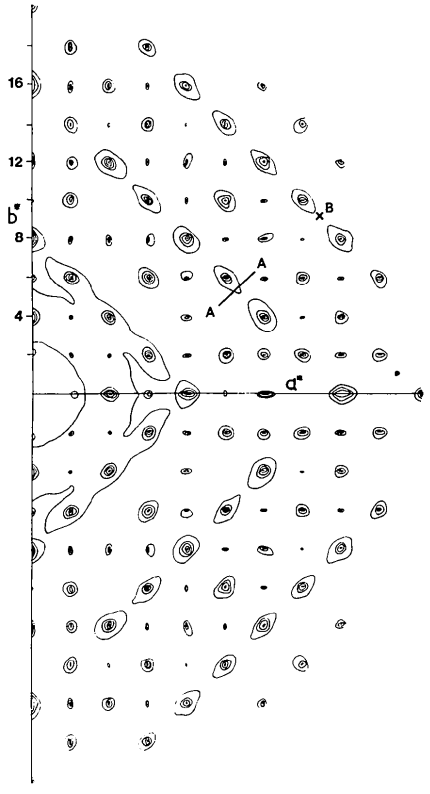

Fig. 6. Diffuse scattering in the *hk*0 reciprocal-lattice plane of DBC.

A more quantitative measurement was made by scanning carefully across the streak passing through 880, along the section *AA*, in order to measure the profile along [110], and vertically through *B* in the 12,12,0 streak to measure the profile along [001]. These sections were chosen so as to be well away from Bragg points and to exclude the effect of any wavelength harmonics from the graphite monochromator that might still get through the pulse-height discrimination of the counting chain. Each point in the profile was measured for 30 min. The profiles were corrected for the effect of the detector slit width by deconvolution by the method of Stokes (1948). No Lorentz–polarization or absorption corrections were applied as these are negligible over the range of measurement.

Figs. 7 and 8 show the profiles obtained. The profiles were analysed in the same way as Singh & Glazer (1981), that is by assuming one-dimensional stacking-type disorder in the [110] and [001] directions to give the streaks along [1$\bar{1}$0]. This is a reasonable approximation because the cross-section of the streaks is very anisotropic and therefore the intensities along the two orthogonal directions across the streaks can be treated as essentially independent. Therefore, for each of these two orthogonal directions the intensity can be described by the Wilson (1962) formula:

$$I = \frac{I_o[1-(1-2\alpha)^2]}{1-2(1-2\alpha)\cos H+(1-2\alpha)^2}$$

for the profile along [110]

$$I = \frac{I_o[1-(1-2\beta)^2]}{1-2(1-2\beta)\cos K+(1-2b)^2}$$

for the profile along [001].

α and β are the probabilities of a mistake in the sequence of structural units along [110] and [001] respectively. $H = 2\pi\mathbf{A}.\mathbf{S}$ and $K = 2\pi\mathbf{B}.\mathbf{S}$, where **A** and **B** are the repeat vectors along the one-dimensional chains in these two directions, and **S** is the appropriate scattering vector in each case. I_o represents intensity derived from the difference in transform of the two disordered species responsible for the diffuse scattering. The above formula was fitted by least squares to the two sets of data, by refining in each case a scale factor, background and α or β appropriately.

For the [110] direction the repeat distance between streaks is $4a^*\sqrt{2}$, as successive streaks pass through the points 440, 880, *etc.* The value of α was determined to be $\alpha = 0{\cdot}122 \pm 0{\cdot}002$, with the theoretical curve shown in Fig. 7.

For the [001] direction the repeat distance between streaks is $8a^*$ and this leads to a least-squares value of $\beta = 0{\cdot}357 \pm 0{\cdot}003$.

These values of α and β can be used to give some idea of the mean domain size *projected* in the appropriate directions. For the [110] direction this is given by $[(1-\alpha)/\alpha] \times$ repeat distance, with a similar formula for β in the [001] direction. For [110] the repeat distance is given by $a/4\sqrt{2}$ and for [001] it is $a/8$.

We calculate the mean projected domain sizes to be $23{\cdot}4 \pm 0{\cdot}5$ Å along [110] and $4{\cdot}1 \pm 0{\cdot}1$ Å along [001] (*cf.* $24{\cdot}5 \pm 0{\cdot}5$ and $4{\cdot}6 \pm 0{\cdot}1$ Å in DBP). Although these values are slightly less than in DBP the differences are probably not significant.

We see then that the type of short-range order in DBC is very similar to that in DBP and again probably corresponds to ordered chiral domains in the same way. Although the difference between the two compounds is in the organic group, this result is not inconsistent with Welberry's view that the cations are the major contributors to the diffuse scattering intensity I_o. It is interesting to see that despite the smaller cation displacements, as suggested by their smaller anisotropic temperature factors compared with DBP, there is a negligible effect on the correlation lengths, pointing again to the earlier suggestion that the degree and direction of correlation is determined principally by the C(3)–C(3)′ intermolecular contacts. It is important to realize that, while the cations are

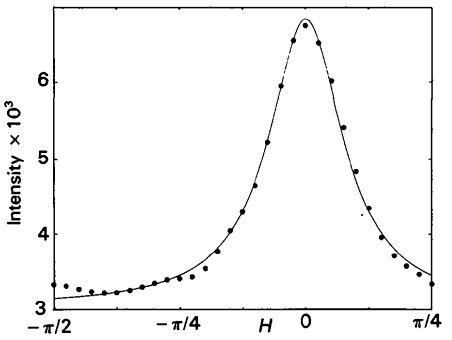

Fig. 7. Section along [110] through the 880 streak: points are experimental measurements; full line is theoretical fit with α = 0·122.

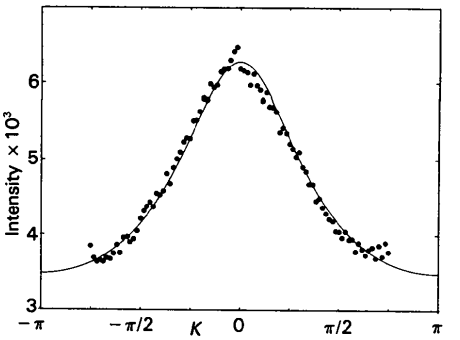

Fig. 8. Section along [001] through 12,12,0 streak: points are experimental measurements; full line is theoretical fit with β = 0·357.

the dominant contributors to the intensity of the diffuse streaks (as shown by Welberry), it is the organic groups which determine the correlation range between the cations, as seen by the fact that the widths of the streaks are very similar in both DBP and DBC.

KS wishes to thank the E. P. Abraham Fund of the University of Oxford for a grant to support this research, and AMG is grateful to the Jagiellonian University for computing facilities and for an invitation to carry out some of this work in Poland.

References

AIZU, K. (1969). *J. Phys. Soc. Jpn*, **27**, 387–396.
BHAT, S. V., DHAR, V. & SRINIVASAN, R. (1982). *Ferroelectrics*, **40**, 49–52.
GLAZER, A. M., STADNICKA, K. & SINGH, S. (1981). *J. Phys. C*, **14**, 5011–5029.
International Tables for X-ray Crystallography (1974). Vol. IV. Birmingham: Kynoch Press.
LUHAN, P. A. & MCPHAIL, A. T. (1972). *J. Chem. Soc. Perkin Trans.* 2, p. 2372.
NAKAMURA, N., SUGA, H., CHIHARA, H. & SEKI, S. (1968). *Bull Chem. Soc. Jpn*, **38**, 291–296.
SHELDRICK, G. M. (1976). *SHELX76*. A program for crystal structure determination. Univ. of Cambridge, England.
SINGH, S. & GLAZER, A. M. (1981). *Acta Cryst.* A**37**, 804–808.
SINGH, S. & WONDRE, F. (1984). *Phase Transitions*. In the press.
STADNICKA, K. & GLAZER, A. M. (1980). *Acta Cryst.* B**36**, 2977–2985.
STADNICKA, K. & GLAZER, A. M. (1982). *Phase Transitions*, **2**, 293–308.
STADNICKA, K., GLAZER, A. M., SINGH, S. & ŚLIWIŃSKI, J. (1982). *J. Phys. C*, **15**, 2577–2586.
STOKES, A. R. (1948). *Proc. Phys. Soc.* **61**, 382–391.
WELBERRY, T. R. (1982) *Acta Cryst.* B**38**, 1921–1927.
WILSON, A. J. C. (1962). *X-ray Optics*. London: Methuen.

Acta Cryst. (1984). B**40**, 145–150

An Application of the Powder-Pattern-Fitting Technique to the Structure Determination of One-Dimensionally Oriented Fibrous Crystals: The Structure of Tetrakis(dimethylammonium) Hexamolybdate(VI) Dihydrate

BY H. TORAYA AND F. MARUMO

Research Laboratory of Engineering Materials, Tokyo Institute of Technology, Nagatsuta 4259, *Yokohama* 227, *Japan*

AND T. YAMASE

Research Laboratory of Resources Utilization, Tokyo Institute of Technology, Nagatsuta 4259, *Yokohama* 227, *Japan*

(*Received* 29 *July* 1983; *accepted* 12 *September* 1983)

Abstract

$[(CH_3)_2NH_2]_4Mo_6O_{20}.2H_2O$ is monoclinic, space group $P2_1$, with $a = 19{\cdot}800\,(8)$, $b = 10{\cdot}294\,(2)$, $c = 7{\cdot}605\,(3)$ Å, $\beta = 90{\cdot}68\,(4)°$, $V = 1549{\cdot}9\,(9)$ Å^3, $Z = 2$ and $D_x = 2{\cdot}39$ g cm^{-3}. It crystallizes in the form of a bundle composed of a number of fibrous crystals having their c axes along the needle axis. The constituent crystals are in completely random orientation around the needle axis. The crystal structure has been determined from photographic intensity data collected with a polycrystalline needle in the equi-inclination Weissenberg geometry around the needle axis. The pattern-fitting technique was applied to obtain structure factors of overlapping reflections. The structure was refined to a final R value of 0·15 for 944 reflections. The structure is composed of infinite chains of polymolybdate anions, $[Mo_6O_{20}^{4-}]_\infty$, running along the c axis, dimethylammonium cations and water molecules, connecting the chains laterally. $[Mo_6O_{20}^{4-}]_\infty$ is a new type of isopolymolybdate anion.

0108-7681/84/020145-06$01.50

Introduction

Alkylammonium polymolybdates(VI) and polytungstates(VI) have received considerable attention in view of their interesting photochemical properties. Recent findings on their ability to photoelectrolyze water stimulated extensive studies on the crystal and molecular structures and photoreactivity of polymolybdate complexes in their +6 oxidation state. We have already reported some aspects of structures, photoreduction (Mo^{VI} to Mo^{V}) properties, and application to water decomposition (Isobe, Marumo, Yamase & Ikawa, 1978; Yamase, 1978; Yamase, Ikawa, Ohhashi & Sasada, 1979; Yamase & Ikawa, 1979, 1980; Yamase, Sasaki & Ikawa, 1981). As part of a systematic study, we synthesized crystals of the title compound, which shows excellent photochromic property (Yamase, Ikawa, Kokado & Inoue, 1973; Yamase & Ikawa, 1974; Arnaud-New & Schwing-Weill, 1973). We then attempted to analyze the crystal structure with particular interest in elucidating the